

RESEARCH ARTICLE | *Liver and Biliary Tract Physiology/Pathophysiology*

Hepatic transcriptome signatures in patients with varying degrees of nonalcoholic fatty liver disease compared with healthy normal-weight individuals

Malte P. Suppli,^{1*} Kristoffer T. G. Rigbolt,^{2*} Sanne S. Veidal,² Sara Heebøll,³ Peter Lykke Eriksen,³ Mia Demant,¹ Jonatan I. Bagger,¹ Jens Christian Nielsen,² Denise Oró,² Sebastian W. Thrane,² Asger Lund,¹ Charlotte Strandberg,⁴ Merete J. Kønig,⁴ Tina Vilsbøll,^{1,5} Niels Vrang,² Karen L. Thomsen,³ Henning Grønbaek,³ Jacob Jelsing,² Henrik H. Hansen,² and Filip K. Knop^{1,5,6}

¹Department of Clinical Metabolic Physiology, Steno Diabetes Center Copenhagen, Gentofte Hospital, University of Copenhagen, Hellerup, Denmark; ²Gubra, Hørsholm, Denmark; ³Department of Hepatology and Gastroenterology, Aarhus University Hospital, Aarhus, Denmark; ⁴Department of Radiology, Gentofte Hospital, University of Copenhagen, Hellerup, Denmark; ⁵Department of Clinical Medicine, Faculty of Health and Medical Sciences, University of Copenhagen, Copenhagen, Denmark; and ⁶Novo Nordisk Foundation Center for Basic Metabolic Research, Faculty of Health and Medical Sciences, University of Copenhagen, Copenhagen, Denmark

Submitted 2 November 2018; accepted in final form 11 January 2019

Suppli MP, Rigbolt KT, Veidal SS, Heebøll S, Eriksen PL, Demant M, Bagger JI, Nielsen JC, Oró D, Thrane SW, Lund A, Strandberg C, Kønig MJ, Vilsbøll T, Vrang N, Thomsen KL, Grønbaek H, Jelsing J, Hansen HH, Knop FK. Hepatic transcriptome signatures in patients with varying degrees of nonalcoholic fatty liver disease compared with healthy normal-weight individuals. *Am J Physiol Gastrointest Liver Physiol* 316: G462–G472, 2019. First published January 17, 2019; doi:10.1152/ajpgi.00358.2018.—Nonalcoholic fatty liver disease (NAFLD) represents a spectrum of conditions ranging from simple steatosis (NAFL), over nonalcoholic steatohepatitis (NASH) with or without fibrosis, to cirrhosis with end-stage disease. The hepatic molecular events underlying the development of NAFLD and transition to NASH are poorly understood. The present study aimed to determine hepatic transcriptome dynamics in patients with NAFL or NASH compared with healthy normal-weight and obese individuals. RNA sequencing and quantitative histomorphometry of liver fat, inflammation and fibrosis were performed on liver biopsies obtained from healthy normal-weight ($n = 14$) and obese ($n = 12$) individuals, NAFL ($n = 15$) and NASH ($n = 16$) patients. Normal-weight and obese subjects showed normal liver histology and comparable gene expression profiles. Liver transcriptome signatures were largely overlapping in NAFL and NASH patients, however, clearly separated from healthy normal-weight and obese controls. Most marked pathway perturbations identified in both NAFL and NASH were associated with markers of lipid metabolism, immunomodulation, extracellular matrix remodeling, and cell cycle control. Interestingly, NASH patients with positive Sonic hedgehog hepatocyte staining showed distinct transcriptome and histomorphometric changes compared with NAFL. In conclusion, application of immunohistochemical markers of hepatocyte injury may serve as a more objective tool for distinguishing NASH from NAFL, facilitating improved resolution of hepatic molecular changes associated with progression of NAFLD.

NEW & NOTEWORTHY Nonalcoholic fatty liver disease (NAFLD) is the most common liver disease in Western countries. NAFLD is associated with the metabolic syndrome and can progress to the more serious form, nonalcoholic steatohepatitis (NASH), and ultimately lead to irreversible liver damage. Using gold standard molecular and histological techniques, this study demonstrates that the currently used diagnostic tools are problematic for differentiating mild NAFLD from NASH and emphasizes the marked need for developing improved histological markers of NAFLD progression.

histomorphometry; nonalcoholic fatty liver disease; nonalcoholic steatohepatitis; transcriptomics

INTRODUCTION

Nonalcoholic fatty liver disease (NAFLD) is an umbrella term that comprises a continuum of liver conditions ranging from simple steatosis, known as nonalcoholic fatty liver (NAFL), to its more aggressive manifestation, nonalcoholic steatohepatitis (NASH). While NAFL has a relatively benign course, patients with NASH are at increased risk of developing liver fibrosis, which can progress to cirrhosis, hepatocellular cancer, and end-stage liver disease (16, 32, 43). As consequence, NASH carries a poor prognosis and constitutes an increasingly frequent reason for liver transplantation (16, 51). The pathogenesis of NAFLD is closely associated with the metabolic syndrome (47, 57), also being an important driver of cardiovascular complications and overall mortality in patients with NAFLD (1, 24). As the globalization of NAFLD runs in close parallel to obesity and type 2 diabetes (53), and therapeutic advances have been slow, the burden of NAFLD has become a major public health issue.

Given the lack of reliable noninvasive surrogate markers, the diagnosis of NASH rests on histomorphological criteria defined by liver biopsy-proven hepatocellular steatosis, lobular inflammation, and evidence of hepatocyte injury such as ballooning degeneration (5, 8). Presence of fibrosis is a sign of chronic inflammation-induced liver injury and represents the

* M. P. Suppli and K. T. G. Rigbolt contributed equally to this work.

Address for reprint requests and other correspondence: F. K. Knop, Clinical Metabolic Physiology, Steno Diabetes Center Copenhagen, Gentofte Hospital, Univ. of Copenhagen, Kildegårdsvej 28, DK-2900, Hellerup, Denmark (e-mail: filip.krag.knop.01@regionh.dk).

strongest predictor of long-term outcomes in NASH (2, 12). The pathogenesis of NASH is complex and considered multifactorial. A number of ‘multiple hit’ hypotheses have been proposed that describe both parallel and sequential molecular mechanisms leading to NASH in the setting of risk factors such as obesity and type 2 diabetes (7, 40). Accordingly, defective lipid metabolism, mounting lipotoxicity, oxidative stress, and immune imbalances have all been linked to NAFLD progression, but the relationships among the various manifestations of NAFLD pathology are poorly understood. Importantly, delineation of molecular signaling patterns specific to disease progression may provide a basis for unraveling the mechanism triggering the transition from NAFL to NASH and eventually the development of targeted and effective treatments for NASH.

Genomewide mapping of gene expression in tissue biopsies has proved valuable for identifying novel diagnostic, prognostic, and therapeutic markers in various diseases, particularly cancer (48). In contrast, advances in hepatic gene signature classifiers for NASH have been slow, and gene transcription programs associated with progression of the disease have therefore not been characterized in detail. The interpretation of available gene expression data is further complicated by the different transcriptomics technologies and control group conditions applied. To date, most insight into liver transcriptome changes in NAFLD has been based on microarray platforms of preselected genes (3, 35, 45, 50, 52, 54, 55). Next-generation sequencing methods, including RNA sequencing, provide hypothesis-free and comprehensive detection of transcribed genes with increased sensitivity, specificity, and broader dynamic range. However, there has been a paucity of liver whole-transcriptome studies in NASH, and next-generation sequencing has therefore only very recently emerged as a powerful tool for addressing molecular mechanisms in NAFLD (10, 15, 17, 22, 44). Notably, there is a marked lack of studies addressing hepatic gene expression signatures in NAFLD subtypes consistent with the spectrum of disease progression. The interpretation of hepatic molecular changes in NAFLD is further challenged by the various indecisive control specimens applied (41, 42, 45, 54, 55), making unresolved the degree to which the liver transcriptome differs between patients with NAFLD and healthy control individuals.

With the aim of clarifying changes in hepatic signaling pathways in NAFLD and the molecular mechanisms underlying progression of the disease, this study investigates the transcriptome signature and quantitative histological markers in liver biopsies, covering the full spectrum from healthy normal-weight and obese individuals over individuals with NAFL to patients with NASH.

METHODS

Individuals

Healthy normal-weight [$n = 14$, body mass index (BMI) 18.5–25 kg/m²] and overweight ($n = 12$, BMI 30–40 kg/m²) participants were recruited at the Center for Diabetes Research, Gentofte Hospital (University of Copenhagen, Hellerup, Denmark). NAFLD patients ($n = 31$) were screened, diagnosed, and recruited at the Department of Hepatology and Gastroenterology, Aarhus University Hospital (Aarhus, Denmark), as described in detail previously (20). NAFLD was diagnosed on the basis of ultrasonographic evidence of hepatic steatosis, elevated liver enzymes, and compatible liver histology. For all

participants, exclusion criteria included diabetes and excessive alcohol intake (>20/12 g/day for men/women). Patients with known diabetes were excluded to avoid the confounding influence of long-term hyperglycemia or antidiabetic medications. All participants gave written informed consent before inclusion. The study protocol conformed to the ethics guidelines of the 1975 Declaration of Helsinki, as reflected in the approvals by the Research Ethics Committee of the Capital Region of Denmark (H-6-2014-097), the Danish National Committee on Health Research Ethics (20110132; 1-10-72-140-14), and the Danish Data Protection Agency (GEH-2014-049; 1-16-02-471-14; 1-16-02-322-15).

Biochemical and Histopathological Evaluation

All included participants underwent a liver biopsy for histological evaluation. Percutaneous liver biopsy was performed under ultrasound guidance. The liver biopsy was divided into a >10-mm sample (portal tracks >10) and fixed in buffered formalin for histological evaluation. The remaining sample material was placed in RNAlater (ThermoFisher Scientific, Waltham, MA) or snap-frozen in liquid nitrogen and stored at –80°C until later processing. Biochemical analyses were applied to fasting blood samples and included alanine aminotransferase and aspartate aminotransferase.

Liver biopsy sections were stained with hematoxylin-eosin (H&E) and Masson’s trichrome. Semiquantitative histopathological scoring and differentiation between normal liver tissue, NAFL ($n = 15$ patients), and NASH ($n = 16$ patients) were performed in a blinded manner by board-certified, experienced histopathologists according to steatosis, activity, and fibrosis (SAF) (6), and Kleiner fibrosis stage (F0–4) (25).

RNA Sequencing

Liver transcriptome analysis was performed by RNA sequencing of RNA extracts from liver biopsy samples, as described in detail elsewhere (26). Only samples of high-quality RNA (RNA integrity number ≥ 7.5) were used in the mRNA sample preparation for sequencing. RNA sequencing libraries were prepared with NeoPrep (Illumina, San Diego, CA) using an Illumina TruSeq Stranded mRNA Library kit for NeoPrep (Illumina) and sequenced on a NextSeq 500 (Illumina) with a NSQ 500 hi-Output KT v.2 (75 CYS, Illumina). Reads were mapped to the GRCh38.p10 Ensembl human genome using STAR v.2.5.2a with default parameters, and the corresponding read counts were corrected for batch effects from sample collection sites in the cohorts containing NAFL/NASH patients by using the R package Limma (39). The R package DESeq2 v.1.18.1 (30) was used for differential expression analysis, P values were adjusted using the Benjamini-Hochberg method, and a cut-off of 0.05 was applied. In the differential expression analysis containing only NAFL and NASH patients, we corrected for sex bias in the regression model using DESeq2.

Functional Annotation of Differentially Expressed Genes

An in-house database of candidate genes associated with NAFLD and fibrosis (Supplementary Table S1; supplemental material for this article is available online at the Journal website) was used to annotate genes involved in NAFLD progression against the control groups. In the comparison between NASH and NAFL patient groups the Reactome pathway database (13) was used for functional annotation in a gene set analysis using the R package PIANO v.1.18.1 (49), with the Stouffer method and Benjamini-Hochberg-adjusted P values.

Histology

Liver biopsy samples were paraffin embedded, sectioned, and stained with H&E (Dako, Glostrup, Denmark), anti-galectin-3 (Biologend, San Diego, CA), Picro-Sirius red (PSR, Sigma-Aldrich, Broendby, Denmark), anti-cytokeratin 8/18 (CK-8/18; Leica Biosys-

Table 1. *Biometrics and blood biochemistry*

Group	n	M/W	Age, yr	Height, cm	Weight, kg	BMI, kg/m ²	ALT, U/l	AST, U/l
Normal-weight controls	14	14/0	39.5 ± 12.0	181.7 ± 5.4	76.6 ± 7.6	23.1 ± 1.6	31.8 ± 8.9	33.4 ± 9.0
Obese controls	12	12/0	36.6 ± 10.2	186.8 ± 8.1	115.2 ± 12.1	33.2 ± 1.3	39.7 ± 15.8	41.2 ± 15.4
NAFL	15	9/6	39.4 ± 10.6	173.9 ± 9.4	98.9 ± 15.3	32.8 ± 5.1	96.7 ± 55.8	45.1 ± 23.8
NASH	16	12/4	38.9 ± 17.0	173.8 ± 8.9	102.9 ± 22.6	33.9 ± 6/2	115.0 ± 50.0	54.8 ± 20.6

Values are means ± SD. ALT, alanine aminotransferase; AST, aspartate aminotransferase; NAFL, nonalcoholic fatty liver; NASH, nonalcoholic steatohepatitis; M, men; W, women.

tems, Newcastle, UK), or anti-Sonic hedgehog (SHH; Abcam, Cambridge, UK). To prevent batch differences in staining intensities, staining procedures were performed on all samples in one single immunohistochemistry run. All sections were evaluated for SHH-positive and CK-8/18-negative hepatocyte staining by two individual histopathologists. For quantitative analysis of H&E, galectin-3 and PSR, stained liver sections were analyzed using digital imaging software (Visiograph; Visiopharm, Hørsholm, Denmark). Histochemical positive staining area was expressed relative (%) to total tissue sectional area (fractional area). Quantitative histological data were analyzed using GraphPad Prism v.7.03 software (GraphPad, La Jolla, CA), and results are shown as means ± SE. A one-way ANOVA with Dunnett's post hoc test was applied, with $P < 0.05$ considered statistically significant.

RESULTS

Clinical Characteristics

Anthropometric and blood measures are indicated in Table 1. Average BMI (kg/m² ± SD) was 23.1 ± 1.6 (healthy normal-weight controls, $n = 14$), 33.2 ± 1.3 (overweight individuals, $n = 12$), 32.8 ± 4.8 (NAFL patients, $n = 15$), and 33.9 ± 6.2 (NASH patients, $n = 16$) (Table 1). The clinical characteristics for a subset of patients with NAFL and NASH have been reported previously (20).

Liver Histopathological Characteristics

Histopathological scores are indicated in Table 2. Healthy normal-weight and obese individuals had normal liver morphology, with few exceptions showing benign isolated steatosis (normal-weight individual, $n = 1$; obese individuals, $n = 6$). None of the healthy normal-weight and obese individuals had histological evidence of lobular inflammation, hepatocyte ballooning, or fibrosis. Patients diagnosed with NAFL had liver steatosis of varying severity, with most patients (10 of 15) presenting severe steatosis. Almost all patients with NAFL (13 of 15) also showed mild-grade lobular inflammation. Inclusion of NASH patients ($n = 16$) was based on histopathological confirmation of hepatocyte ballooning morphology.

Table 2. *Semiquantitative evaluation of steatosis, lobular inflammation, hepatocellular ballooning, and fibrosis*

Group	n	Steatosis Score				Inflammation Score			Ballooning Score			Fibrosis Stage				
		0	1	2	3	0	1	2	0	1	2	0	1	2	3	4
Normal-weight controls	14	13	1			14			14			14				
Obese controls	12	6	5	1		12			12			12				
NAFL	15		2	3	10	2	13		15			14	1			
NASH	16			2	14		16			10	6	3	12	1		

Histopathology was scored on liver biopsy sections according to criteria outlined by the NASH-Clinical Research Network (25). Differentiation between nonalcoholic fatty liver (NAFL; presence of steatosis in >5% of hepatocytes; activity score <2) and nonalcoholic steatohepatitis (NASH; presence of hepatocyte ballooning; activity score ≥2) was performed using the Steatosis-Activity-Fibrosis (SAF) algorithm (6).

Liver Transcriptome Profiles

Global gene expression patterns. To compare global gene expression profiles in the liver biopsy samples, a principal component analysis (PCA) was performed. The primary PCA, accounting for the major variability in the data set, indicated that liver transcriptome profiles in healthy normal-weight controls and obese individuals clustered together and were clearly separated from the transcriptome profiles in NAFL/NASH patient samples (Fig. 1A). Whereas liver biopsies from NAFL and NASH patients displayed an extensive number of differentially expressed genes (DEGs; $n = 8,244$), a considerably lower number of DEGs ($n = 55$) were detected in obese individuals compared with normal-weight controls (Fig. 1B). For initial validation of the DEGs identified, we probed for candidate gene transcripts associated with NAFLD and fibrosis (see complete list of genes in Supplementary Table S1). None of the preselected genes were significantly regulated in obese control individuals compared with normal-weight controls. In contrast, NAFL/NASH patients showed significant regulations of a large proportion of candidate genes (Fig. 1C). Gene regulations in NAFL and NASH patients were particularly associated with stimulated synthesis of fatty acids (*SCD1*) and cholesterol (*HMGCR*, *HMGCS1*, *HMGCS2*, *SQLE*), increased lipoprotein activity (*LDLR*, *VLDLR*, *SCARB1*), impaired insulin function (*G6PASE*, *INSR*, *IRS1*, *IRS2*, *MEK2*, *PEPCK*, *PRCK1*, *PRKCZ*, *PYG*), increased FXR signaling (*FXR*, *APOCII*, *APOCIII*, *MDR3*, *OAT2*, *OSTB*, *UGT2B4*), modulation of monocyte differentiation and recruitment (*CCR1*, *CD14*, *CD163*, *CD68*, *CD86*, *F4/80*, *LGALS3*, *MCP-1*, *TGFB*), and inflammation signaling (*IKK*, *JNK*, *SMAD3*, *SMAD4*, *TLR4*, *TNFR*, *TRAF6*), proapoptotic activity (*CASP3*, *CASP6*, *CASP7*), and stimulated collagen formation (*A-SMA*, *COL1A1*, *COL1A2*, *COL3A1*).

Liver transcriptome changes in NAFL vs. NASH. To obtain further resolution of liver transcriptome changes in NASH vs. NAFL, a subsequent principal component analysis was performed for group-wise comparison of global gene expression

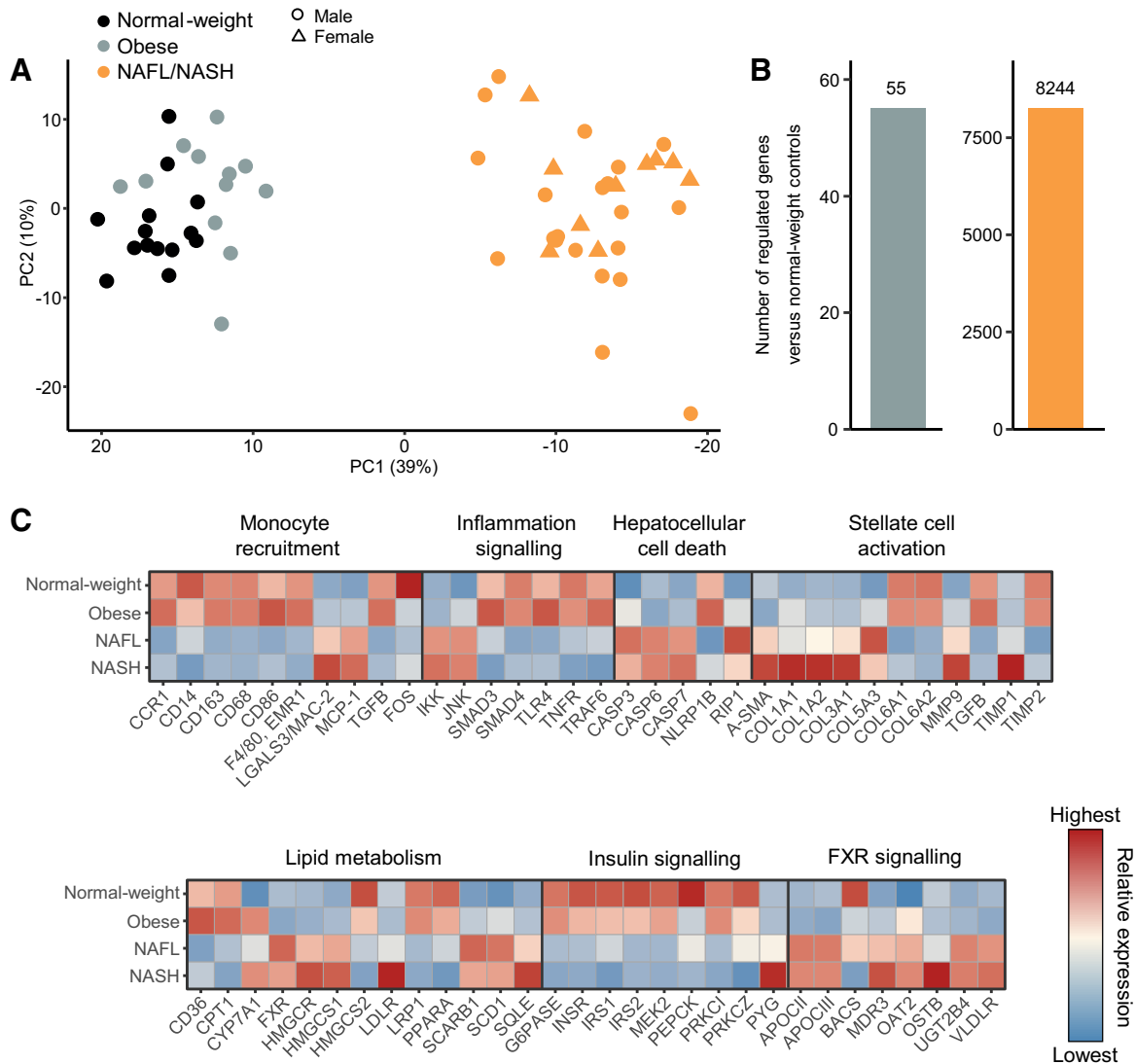


Fig. 1. Overview of hepatic gene expression profiles in healthy normal-weight controls, obese individuals, and nonalcoholic fatty liver/nonalcoholic steatohepatitis (NAFL/NASH) patients. *A*: principal component analysis (PCA) of samples based on the top 500 most variable gene expression levels. *B*: total number of differentially expressed genes (false discovery rate <0.05) in obese individuals and NAFL/NASH patients relative to healthy normal-weight individuals. *C*: relative gene expression levels (z -scores) of significantly regulated NAFLD/fibrosis-associated candidate genes (see Supplemental Table S1 for complete list of in-house gene set). FXR, farnesoid X receptor. PC1, first principal component; PC2, second principal component.

profiles (Fig. 2A). As the two control groups consisted only of male subjects, the statistical analysis was adjusted to account for gender bias when discriminating liver transcriptome changes in NAFL versus NASH patients. Compared with NAFL, a total of 132 genes (upregulated, $n = 112$; downregulated, $n = 20$) were significantly regulated in NASH (Fig. 2B; see Supplemental Table S2 for complete list of DEGs). To get a systematic overview of biological pathway perturbations in NASH versus NAFL, a gene set enrichment analysis was subsequently conducted. The analysis identified a subset of pathways significantly enriched in NASH compared with NAFL (Fig. 2C). Most significantly regulated pathways were extracellular matrix organization (*COL1A2*, *COL4A1*, *COL4A6*, *COL16A1*, *CTSK*, *EFEMP1*, *FBLN5*, *LAMA1*, *LAMC3*, *LTBP2*, *LOXL4*, *MMP23*, *MMP24*, *VCAN*) and immune system (*C5A1*, *CASP1*, *DAPPI*, *GSN*, *EDA*, *MRC2*, *OLR1*, *PLAU*, *RNASE6*, *TMEM173*), see Fig. 2D.

The top 10 significantly regulated genes with increased or decreased expression are indicated in Table 3.

Comparison of liver transcriptome profiles in SHH-positive vs. SHH-negative NASH patients. To facilitate improved detection of hepatocyte degenerative profiles, immunohistochemical markers of hepatocyte injury (SHH, CK-8/18) (17, 35) were applied. Clinical and liver histopathological characteristics of the two NASH subgroups are indicated in Fig. 3A. In NASH patients, most biopsies (11 of 16) showed a clear overlap of SHH-positive and CK-8/18-negative hepatocytes with corresponding hepatocyte ballooning profiles visualized by conventional H&E staining (Fig. 3B). Since SHH-positive staining served as a more objective marker for ballooning hepatocytes in the biopsy samples, this prompted us to compare global gene expression patterns in liver biopsies from NASH patients categorized as SHH positive ($n = 11$) or SHH negative ($n = 5$). NASH biopsies with SHH-positive hepato-

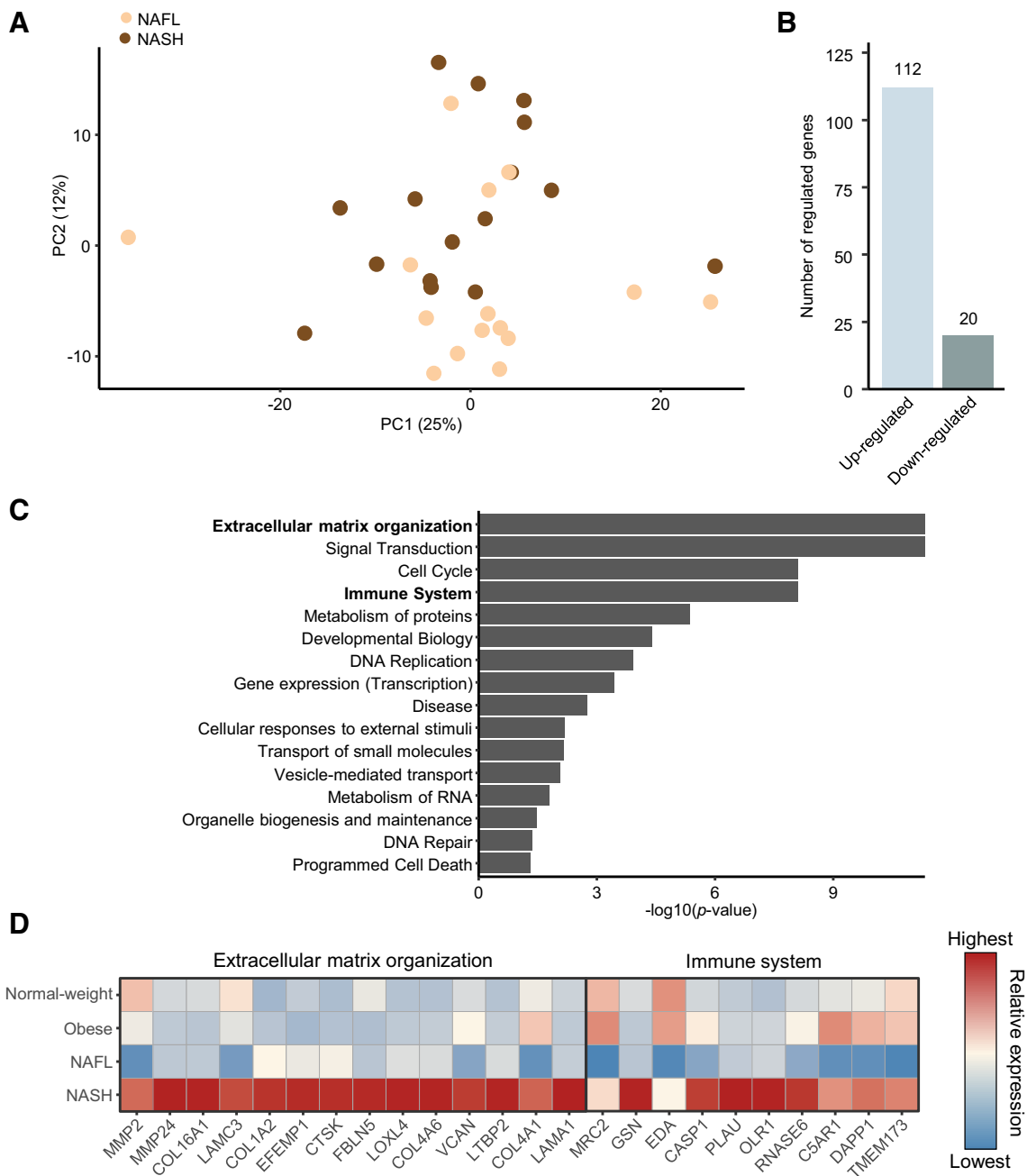


Fig. 2. Gene set analysis of differences in nonalcoholic steatohepatitis (NASH) vs. nonalcoholic fatty liver (NAFL). **A**: principal component analysis of samples based on top 500 most variable gene expression levels. **B**: groupwise comparison of total number of differentially expressed genes (DEGs; false discovery rate <0.05) between NASH and NAFL. DEGs are listed in Supplemental Table S2. **C**: significance level of enrichment of individual gene sets in the Reactome pathway database, indicating regulated pathways in NASH compared with NAFL. **D**: relative gene expression levels (z -scores) of differentially regulated genes in most significantly regulated Reactome pathways (extracellular matrix organization, immune system). In cell cycle pathway, only a single gene was significantly regulated (*CENPU*). A subset of DEGs was represented in both extracellular matrix organization and signal transduction pathways (*COL1A2*, *COL4A1*, *LAMA1*, *MMP2*). Significantly regulated genes specific to signal transduction were *ADORA3*, *AKR1B10*, *C5AR1*, *CNKSR2*, *FGF1*, *FMNL3*, *GPC3*, *GPNMB*, *KLHL12*, *LAMC3*, *MAML2*, *NEURLIB*, *PDE4A*, *RGS16*, *RUNX1*, *ST3GAL6*, and *THBS2*.

cyte staining showed discernible transcriptome changes compared with NAFL ($n = 282$ DEGs; Fig. 3C), including genes associated with extracellular matrix organization and remodeling (*CAPN2*, *COL1A2*, *COL4A1*, *COL4A2*, *COL16A1*, *COL18A1*, *EFEMP1*, *FBLN5*, *LAMC3*, *LOXL4*, *MGP*, *MMP2*, *MMP24*, *PODN*, *TIMP1*, *VCAN*), cell adhesion/tight junction function (*ANTXR1*, *CLDN11*, *EPCAM*), immune modulation (*EDA*, *ELK1*, *IFI16*, *IL17RC*, *LEAP2*, *TNFRSF1A*), cell cycle control (*CENPU*,

MCM4, *MCM6*, *MCM7*, *POLA2*, *SUN2*), apoptosis (*CASP1*, *CYCS*, *GSN*, *PSMC2*), metallothionein family antioxidant proteins (*MT1E*, *MT1F*, *MT1M*, *MT1X*, *MT2A*), and microtubule dynamics (*STMN2*). In contrast, gene expression signatures in SHH-negative NASH patients were virtually identical to those of NAFL patients ($n = 2$ DEGs; *ACSL4*, *GSTM1*). All DEGs detected in the two NASH subgroups are listed in Supplementary Tables S3 and S4 (online only), respectively.

Table 3. Top 10 upregulated and downregulated genes in NASH compared with NAFL

Gene Symbol	Gene Name	P Value	Fold Change NASH vs. NAFL	Function	Reactome Pathway
<i>Upregulated genes</i>					
<i>MMP2</i>	Matrix metalloproteinase 2	4.22E-04	1.97	ECM remodeling	ECM organization
<i>FMNL3</i>	Formin-like 3	1.65E-03	1.58	Cell-cell adhesion, cell proliferation	Signal transduction
<i>OTOA</i>	Otoancorin	1.65E-03	5.51	Cell-cell adhesion	Metabolism of proteins
<i>CPXMI</i>	Carboxypeptidase X, M14 family member 1	1.65E-03	9.31	ECM remodeling	NA
<i>PROCR</i>	Protein C receptor	1.65E-03	1.93	Serine protease, cell proliferation	Hemostasis
<i>MMP24</i>	Matrix metalloproteinase 24	1.65E-03	3.75	ECM remodeling	ECM organization
<i>TNNT1</i>	Troponin T1, slow skeletal type	1.65E-03	35.11	Filament regulatory protein	Muscle contraction
<i>GPC3</i>	Glypican 3	2.21E-03	4.16	Cell proliferation	Metabolism of proteins
<i>ADGRG1</i>	Adhesion G protein-coupled receptor G1	2.21E-03	2.27	Cell-cell adhesion, collagen receptor	NA
<i>MRC2</i>	Mannose receptor C type 2	3.72E-03	1.75	ECM remodeling, cell proliferation	Immune system
<i>Downregulated genes</i>					
<i>SLC25A48</i>	Solute carrier family 25 member 48	1.65E-03	0.14	Transmembrane transport	NA
<i>MT1E</i>	Metallothionein 1E	1.65E-03	0.45	Antioxidant protein	Metallothioneins bind metals
<i>MAT1A</i>	Methionine adenosyltransferase 1A	2.21E-03	0.69	Transmethylation, cell proliferation	Methylation
<i>MT1X</i>	Metallothionein 1X	2.62E-03	0.49	Antioxidant protein	Metallothioneins bind metals
<i>ST3GAL6</i>	ST3 beta-galactoside alpha-2, 3-sialyltransferase 6	7.50E-03	0.71	Cell-cell adhesion, cell proliferation	Metabolism of proteins
<i>C4ORF48</i>	Chromosome 4 open reading frame 48	7.50E-03	0.12	Cell proliferation	NA
<i>ETNK2</i>	Ethanolamine kinase 2	9.91E-03	0.70	Phospholipid synthesis	Metabolism of lipids
<i>ABHD15</i>	Abhydrolase domain containing 15	1.02E-02	0.82	Adipogenesis, lipolysis	NA
<i>MXI1</i>	MAX interactor 1, dimerization protein	1.05E-02	0.72	Potential tumor suppressor	NA
<i>HORMAD2</i>	HORMA domain containing 2	1.77E-02	0.50	Cell proliferation, cell cycle	NA

Genes are ranked according to *P* value. See Supplemental Table S2 for complete list of differentially expressed genes (DEGs). ECM, extracellular matrix; NA, gene pending Reactome database curation.

Quantitative Histology

Assessment of the proportional (fractional) area of liver fat (Fig. 4A) revealed similar marked hepatocellular fat accumulation in patients with NAFL (20.3 ± 2.0 , $P < 0.001$), SHH-negative NASH (21.6 ± 3.3 , $P < 0.001$), and SHH-positive NASH ($24.2 \pm 2.6\%$, $P < 0.001$) compared with normal-weight ($2.9 \pm 0.4\%$) and obese individuals ($5.7 \pm 1.2\%$). Mean fractional areas of galectin-3 staining (Fig. 4B) were similar in normal-weight ($0.1 \pm 0.01\%$) and obese individuals ($0.3 \pm 0.1\%$, $P > 0.05$). Galectin-3 levels tended to be elevated in patients with NAFL ($0.5 \pm 0.1\%$, $P > 0.05$), and SHH-negative NASH (0.7 ± 0.3 , $P > 0.05$), however, was significantly increased only in SHH-positive NASH patients ($1.6 \pm 0.4\%$, $P < 0.001$). Compared with normal-weight individuals, the fractional area of PSR-stained collagen fibers (Fig. 4C) was significantly increased only in individuals with SHH-positive NASH ($3.1 \pm 0.6\%$ vs. $1.7 \pm 0.2\%$, $P < 0.01$).

DISCUSSION

We herein report largely overlapping liver transcriptome signatures in patients diagnosed with NAFL and NASH. Compared with NAFL, NASH patients with positive SHH staining showed distinct transcriptome signature and quantitative histopathological changes. These findings suggest that using only histomorphological criteria (hepatocyte ballooning) for diagnosing NASH may insufficiently separate the two NAFLD subtypes and mask molecular mechanisms involved in the transition from NAFL to NASH.

The liver transcriptome and associated functional annotations were largely overlapping in healthy normal-weight and obese individuals, indicating that obesity did not act as a

confounding factor in the evaluation of disease-associated transcriptome signatures in NAFL and NASH. Gene expression signatures in obese patients with NAFL or NASH were profoundly distinguished from both healthy normal-weight and obese individuals. Considering the extent and diversity of gene expression changes, this suggests widespread alterations in hepatic molecular signaling in NAFL and NASH. Global gene expression profiles in the two NAFLD groups showed a relatively high degree of clustering, indicating a large degree of overlap in liver transcriptome changes, which is consistent with the NASH patients showing relatively low disease severity. Accordingly, several disease-associated candidate genes were differentially expressed in both NAFL and NASH patients. Previous microarray, RNA sequencing, and meta-analysis studies have identified similar gene transcriptional alterations associated with lipid metabolism (*HMGCS2*, *LDLR*, *SCD1*) (3, 55, 58), insulin receptor function/glucose metabolism (*IRS2*, *G6PASE*) (3, 28, 58), farnesoid X receptor (FXR) signaling (*PPARA*) (58), monocyte recruitment (*CD14*, *CD163*) (41, 58), and inflammation signaling (*TGFB*) (28), as well as stellate cell activation and fibrogenesis (*A-SMA*, *COL1A1*, *COL1A2*, *COL3A1*, *COL6A1*, *COL6A2*, *PDGF*) (15, 28, 35, 41, 45, 58), further validating our RNA sequencing data set. An unsupervised analysis was subsequently applied for full-scale mapping of liver transcriptome signatures in NAFL and NASH patients. Because control groups consisted of male subjects only, the comparative analysis of NAFL and NASH patients were corrected for sex bias in the statistical analysis. A signature of 132 genes differentiated NASH patients from those diagnosed with NAFL. Considering the comprehensive gene expression changes in NAFL/NASH

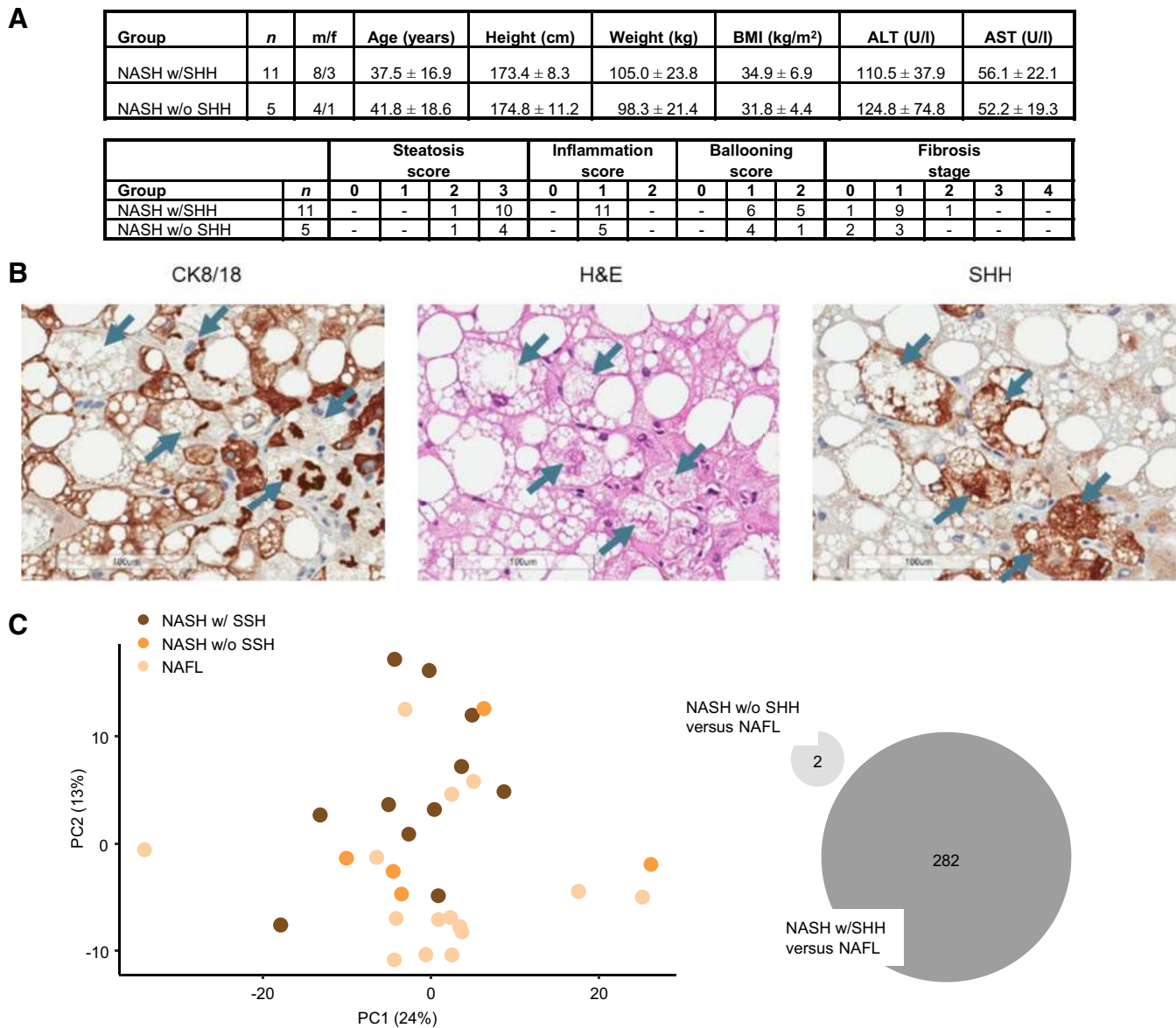


Fig. 3. Liver transcriptome changes in nonalcoholic steatohepatitis (NASH) patients categorized according to presence or absence of Sonic hedgehog (SHH)-positive hepatocyte staining. *A, top*: biometrics and blood biochemistry. Data are expressed as means ± SD; *bottom*: semiquantitative evaluation of steatosis, lobular inflammation, hepatocellular ballooning, and fibrosis. Histopathology was scored on liver biopsy sections according to criteria outlined by the NASH-Clinical Research Network (25). Differentiation between nonalcoholic fatty liver (NAFL; presence of steatosis in >5% of hepatocytes; activity score <2) and NASH (presence of hepatocyte ballooning; activity score ≥2) was performed using the steatosis-activity-fibrosis algorithm (6). *Bottom*: liver biopsy samples categorized according to presence (w/SHH) or absence (w/o SHH) of SHH-positive hepatocytes. *B*: degenerating (ballooning) hepatocyte profiles visualized by conventional hematoxylin-eosin (H&E) staining vs. immunohistochemical detection of cytokeratin-8/18 (CK-8/18, negative staining) and SHH, positive staining). Arrows denote ballooning hepatocyte profiles with both SHH-positive and CK-8/18-negative labeling. *C*: comparison of liver transcriptome profiles in NASH patients with (w/SHH) or without (w/o SHH)-positive hepatocytes. *Left*: principal component analysis of samples based on top 500 most variable gene expression levels in 3 NAFLD subgroups. *Right*: groupwise comparison of total number of differentially expressed genes (DEGs) in NASH patients with or without SHH compared with NAFL (false discovery rate <0.05). For a complete list of DEGs detected in the 2 NASH subgroups, see Supplementary Tables S3 and S4.

compared with healthy normal-weight controls, this further emphasizes the relatively discrete changes in gene expression patterns specific to NASH. Also, the considerable overlap between global liver transcriptome profiles associated with the two NAFLD subtypes supports the concept that a continuum of interacting molecular mechanisms and signaling pathways drives the transition from NAFL to NASH (7, 34, 36, 40). Pathway perturbations identified in NASH patients were most consistently linked to mechanisms of immune function and extracellular matrix remodeling.

In addition to changes in NAFLD-associated candidate genes, we confirmed regulation of previously reported genes associated with extracellular matrix interaction (*AEBP1*, *DPT*, *EFEMP1*, *FBLN5*, *ITGBL1*, *LOXLA*, *THBS2*, *VCAN*), cell division/carcinogenesis (*AKR1B10*, *CIORF198*, *GPC3*), apoptosis (*PNMA1*), and transmethylation activity (*MATIA*) (3, 35, 45). The extensive regulation of extracellular matrix-associated genes therefore indicates that a major difference between liver transcriptome profiles in NAFL and NASH was attributed to the histopathological evidence of fibrosis and not NASH per se.

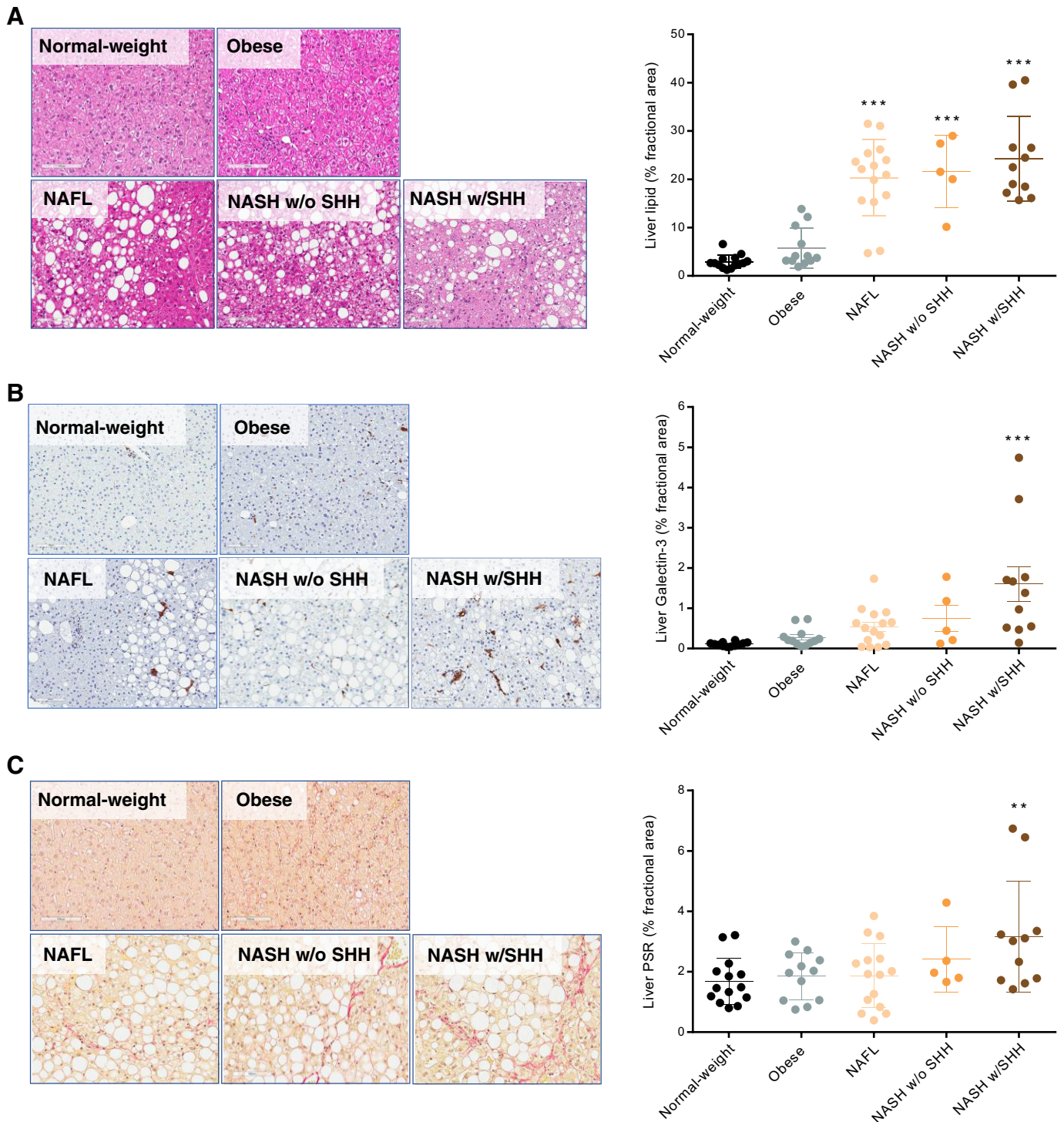


Fig. 4. Imaging-based quantitative histochemical analysis. *A*: liver fat. *B*: galectin-3 immunopositive inflammatory cells. *C*: collagen deposition. Data are expressed as proportional (%fractional) area stained for liver fat (hematoxylin-eosin staining), galectin-3 (immunostaining), and collagen (Picro-Sirius red staining). ** $P < 0.01$, *** $P < 0.001$ vs. healthy normal-weight controls.

Hepatocyte ballooning is considered a defining hallmark of NAFL progression to NASH (6, 9, 25, 33). Nevertheless, the term is ill defined and may be associated with weak intra- and interobserver agreement, which can lead to significant differences in the grading of NAFLD severity and interpretation of treatment outcome (6, 23, 25, 56). Reconciling this issue may

potentially be facilitated with the additional use of immunohistochemical markers of hepatocyte injury, such as SHH (18, 38) and CK-8/18 (19, 27). We therefore performed a scrutinized analysis of hepatocyte injury profiles visualized by different staining procedures. Conventional H&E staining revealed variable distinctiveness of hepatocyte ballooning degen-

eration in liver biopsies from NASH patients. In contrast, hepatocyte injury profiles were more clearly and unequivocally detected when determined by SHH or CK-8/18 immunostaining. Aberrant activation of hedgehog signaling has been implicated in various liver conditions such as inflammation, fibrosis, and hepatocarcinogenesis (11, 37, 46). Conversely, a reduced number of SHH-positive hepatocytes has been associated with improved NAFLD prognosis (18). Compared with NAFL, gene expression changes could be detected in NASH patients only when also accounting for SHH-positive hepatocyte staining. This distinction resulted in the identification of extensive liver transcriptome changes in SHH-positive NASH patients, including genes previously reported regulated in NASH but not, however, detected in our initial analyses (*ANTRX1*, *CLDN11*, *EPCAM*, *MGP*, *PODN*, *STMN2*) (3, 35, 45).

Because histopathological disease scoring systems are inherently semiquantitative, we also determined disease-associated liver histological changes by quantitative means using imaging-based histomorphometry. Biopsies from NAFL and NASH patients with or without SHH-positive staining showed comparable marked increases in the proportionate area of fat, likely reflecting that almost all NAFLD patients regardless of disease subtype showed moderate- to severe-grade steatosis determined by histopathological scoring. Corresponding to the histomorphological evaluation of fibrosis, quantitative analysis of PSR staining revealed increased collagen deposition only in NASH, but not in NAFL, patients. As PSR binds to various collagen isoforms (4), this confirms our RNA sequencing data that several collagen subtypes contribute to increased collagen formation during NAFLD progression. Although lobular inflammation scores were similar in patients with NAFL and NASH, only NASH patients showed a significantly elevated proportionate area of galectin-3 staining and increased galectin-3 mRNA expression. Galectin-3 is produced by several immune cell phenotypes, in particular, activated macrophages and lymphocytes (21, 29), and quantitative histomorphology may therefore provide a more accurate measure of hepatic immune cell activation that is not accounted for when using histopathological scoring criteria. Significant quantitative changes in galectin-3 and PSR staining were observed only in NASH patients with SHH-positive hepatocyte staining, being in good agreement with the robust gene expression signature of aberrant immune function and enhanced fibrogenesis in this subgroup.

Although the numbers of NAFL and NASH patients were small, our observation that only SHH-positive samples showed a discriminatory liver transcriptome and histomorphometric signature compared with NAFL invites the possibility that application of additional histological markers of hepatocyte damage may enable further resolution of molecular changes associated with the progression of NAFLD. The number of SHH-positive cells is reported to correlate with the severity of NASH (18, 31). Our observation that most, but not all, liver biopsies from NASH patients showed SHH-positive hepatocytes may therefore tentatively be ascribed to individual differences in disease progression. Limitations in the present study should be considered. Immunohistochemical stainings were performed on different biopsy sections than those used for diagnosing NASH, preventing direct comparison of SHH staining with corresponding individual diagnostic hepatocyte

ballooning profiles. It should also be noted that the present study is limited to describing hepatic molecular changes in NASH patients with relatively low disease severity, necessitating future studies on larger patient cohorts representing different stages of NASH. Furthermore, as control groups consisted of males only, it also remains to be addressed in detail how sex differences may potentially influence gene expression profiles in NAFL vs. NASH. In addition, study subjects were nondiabetic and were evaluated only for hepatic markers; hence, the study conditions do not capture the extent of extrahepatic molecular changes involved in the pathogenesis and progression of NAFLD (14).

Conclusions

Liver transcriptome signatures and quantitative changes in histopathological markers were largely similar in NAFL and NASH patients; however, they markedly differed from both healthy normal-weight and obese control individuals. Compared with NAFL, most marked differences in transcriptome signatures and quantitative histopathological changes mapped to proinflammatory and fibrogenesis-associated mechanisms. As extensive molecular changes were specifically identified in NASH patients with SHH-positive hepatocyte staining, this suggests the utility of applying immunohistochemical markers of hepatocyte injury as a more objective diagnostic modality in the distinction between NAFL and NASH.

GRANTS

This study received funding from the Novo Nordisk Foundation, the A.P. Møller Foundation, and the Jacob and Olga Madsen Foundation.

DISCLOSURES

No conflicts of interest, financial or otherwise, are declared by the authors.

AUTHOR CONTRIBUTIONS

J.I.B., A.L., N.V., H.G., J.J., and F.K.K. conceived and designed research; M.P.S., K.T.G.R., S.S.V., S.H., P.L.E., M.D., J.I.B., D.O., S.W.T., C.S., and K.L.T. performed experiments; M.P.S., K.T.G.R., S.S.V., S.H., P.L.E., M.D., J.I.B., J.C.N., D.O., S.W.T., A.L., C.S., M.J.K., T.V., K.L.T., H.G., J.J., H.H.H., and F.K.K. analyzed data; K.T.G.R., S.S.V., P.L.E., J.C.N., D.O., S.W.T., A.L., M.J.K., T.V., N.V., K.L.T., H.G., J.J., H.H.H., and F.K.K. interpreted results of experiments; K.T.G.R., S.S.V., J.C.N., D.O., S.W.T., and H.H.H. prepared figures; K.T.G.R., S.S.V., S.H., J.C.N., H.G., J.J., H.H.H., and F.K.K. drafted manuscript; M.P.S., K.T.G.R., P.L.E., J.C.N., K.L.T., H.G., J.J., H.H.H., and F.K.K. edited and revised manuscript; M.P.S., K.T.G.R., S.S.V., S.H., P.L.E., M.D., J.I.B., J.C.N., D.O., S.W.T., A.L., C.S., M.J.K., T.V., N.V., K.L.T., H.G., J.J., H.H.H., and F.K.K. approved final version of manuscript.

REFERENCES

- Allen AM, Therneau TM, Larson JJ, Coward A, Somers VK, Kamath PS. Nonalcoholic fatty liver disease incidence and impact on metabolic burden and death: A 20 year-community study. *Hepatology* 67: 1726–1736, 2018. doi:10.1002/hep.29546.
- Angulo P, Kleiner DE, Dam-Larsen S, Adams LA, Bjornsson ES, Charatcharoenwithaya P, Mills PR, Keach JC, Lafferty HD, Stahler A, Haffadottir S, Bendtsen F. Liver fibrosis, but no other histologic features, is associated with long-term outcomes of patients with nonalcoholic fatty liver disease. *Gastroenterology* 149: 389–97.e10, 2015. doi:10.1053/j.gastro.2015.04.043.
- Arendt BM, Comelli EM, Ma DWL, Lou W, Teterina A, Kim T, Fung SK, Wong DKH, McGilvray I, Fischer SE, Allard JP. Altered hepatic

- gene expression in nonalcoholic fatty liver disease is associated with lower hepatic n-3 and n-6 polyunsaturated fatty acids. *Hepatology* 61: 1565–1578, 2015. doi:10.1002/hep.27695.
4. **Armendáriz-Borunda J, Rojkind M.** A simple quantitative method for collagen typing in tissue samples: its application to human liver with schistosomiasis. *Coll Relat Res* 4: 35–47, 1984. doi:10.1016/S0174-173X(84)80027-8.
 5. **Bedossa P.** Pathology of non-alcoholic fatty liver disease. *Liver Int* 37, Suppl 1: 85–89, 2017. doi:10.1111/liv.13301.
 6. **Bedossa P, Poitou C, Veyrie N, Bouillot J-L, Basdevant A, Paradis V, Tordjman J, Clement K.** Histopathological algorithm and scoring system for evaluation of liver lesions in morbidly obese patients. *Hepatology* 56: 1751–1759, 2012. doi:10.1002/hep.25889.
 7. **Berlanga A, Guin-Jurado E, Porras JA, Auguet T.** Molecular pathways in non-alcoholic fatty liver disease. *Clin Exp Gastroenterol* 7: 221–239, 2014. doi:10.2147/CEG.S62831.
 8. **Brown GT, Kleiner DE.** Histopathology of nonalcoholic fatty liver disease and nonalcoholic steatohepatitis. *Metabolism* 65: 1080–1086, 2016. doi:10.1016/j.metabol.2015.11.008.
 9. **Caldwell S, Ikura Y, Dias D, Isomoto K, Yabu A, Moskaluk C, Pramoonjago P, Simmons W, Scruggs H, Rosenbaum N, Wilkinson T, Toms P, Argo CK, Al-Osaimi AMS, Redick JA.** Hepatocellular ballooning in NASH. *J Hepatol* 53: 719–723, 2010. doi:10.1016/j.jhep.2010.04.031.
 10. **Chu X, Jin Q, Chen H, Wood GC, Petrick A, Strodel W, Gabrielsen J, Benotti P, Mirshahi T, Carey DJ, Still CD, DiStefano JK, Gerhard GS.** CCL20 is up-regulated in non-alcoholic fatty liver disease fibrosis and is produced by hepatic stellate cells in response to fatty acid loading. *J Transl Med* 16: 108, 2018. doi:10.1186/s12967-018-1490-y.
 11. **Chung SI, Moon H, Ju H-L, Cho KJ, Kim DY, Han K-H, Eun JW, Nam SW, Ribback S, Dombrowski F, Calvisi DF, Ro SW.** Hepatic expression of Sonic Hedgehog induces liver fibrosis and promotes hepatocarcinogenesis in a transgenic mouse model. *J Hepatol* 64: 618–627, 2016. doi:10.1016/j.jhep.2015.10.007.
 12. **Ekstedt M, Hagström H, Nasr P, Fredrikson M, Stål P, Kechagias S, Hultcrantz R.** Fibrosis stage is the strongest predictor for disease-specific mortality in NAFLD after up to 33 years of follow-up. *Hepatology* 61: 1547–1554, 2015. doi:10.1002/hep.27368.
 13. **Fabregat A, Jupe S, Matthews L, Sidiropoulos K, Gillespie M, Garapati P, Haw R, Jassal B, Korninger F, May B, Milacic M, Roca CD, Rothfels K, Sevilla C, Shamovsky V, Shorsler S, Varusai T, Viteri G, Weiser J, Wu G, Stein L, Hermjakob H, D'Eustachio P.** The reactome pathway knowledgebase. *Nucleic Acids Res* 46, D1: D649–D655, 2018. doi:10.1093/nar/gkx1132.
 14. **Friedman SL, Neuschwander-Tetri BA, Rinella M, Sanyal AJ.** Mechanisms of NAFLD development and therapeutic strategies. *Nat Med* 24: 908–922, 2018. doi:10.1038/s41591-018-0104-9.
 15. **Gerhard GS, Legendre C, Still CD, Chu X, Petrick A, DiStefano JK.** Transcriptomic profiling of obesity-related nonalcoholic steatohepatitis reveals a core set of fibrosis-specific genes. *J Endocr Soc* 2: 710–726, 2018. doi:10.1210/je.2018-00122.
 16. **Goldberg D, Ditah IC, Saeian K, Lalehzari M, Aronsohn A, Gorospe EC, Charlton M.** Changes in the prevalence of hepatitis C virus infection, nonalcoholic steatohepatitis, and alcoholic liver disease among patients with cirrhosis or liver failure on the waitlist for liver transplantation. *Gastroenterology* 152: 1090–1099.e1, 2017. doi:10.1053/j.gastro.2017.01.003.
 17. **Guo Y, Xiong Y, Sheng Q, Zhao S, Wattacheril J, Flynn CR.** A micro-RNA expression signature for human NAFLD progression. *J Gastroenterol* 51: 1022–1030, 2016. doi:10.1007/s00535-016-1178-0.
 18. **Guy CD, Suzuki A, Abdelmalek MF, Burchette JL, Diehl AM; NASH CRN.** Treatment response in the PIVENS trial is associated with decreased Hedgehog pathway activity. *Hepatology* 61: 98–107, 2015. doi:10.1002/hep.27235.
 19. **Guy CD, Suzuki A, Burchette JL, Brunt EM, Abdelmalek MF, Cardona D, McCall SJ, Unalp A, Belt P, Ferrell LD, Diehl AM; Nonalcoholic Steatohepatitis Clinical Research Network.** Costaining for keratins 8/18 plus ubiquitin improves detection of hepatocyte injury in nonalcoholic fatty liver disease. *Hum Pathol* 43: 790–800, 2012. doi:10.1016/j.humpath.2011.07.007.
 20. **Heebøll S, Kreuzfeldt M, Hamilton-Dutoit S, Kjær Poulsen M, Stød-kilde-Jørgensen H, Møller HJ, Jessen N, Thorsen K, Kristina Hellberg Y, Bønløkke Pedersen S, Grønbæk H.** Placebo-controlled, randomised clinical trial: high-dose resveratrol treatment for non-alcoholic fatty liver disease. *Scand J Gastroenterol* 51: 456–464, 2016. doi:10.3109/00365521.2015.1107620.
 21. **Henderson NC, Sethi T.** The regulation of inflammation by galectin-3. *Immunol Rev* 230: 160–171, 2009. doi:10.1111/j.1600-065X.2009.00794.x.
 22. **Hotta K, Kikuchi M, Kitamoto T, Kitamoto A, Ogawa Y, Honda Y, Kessoku T, Kobayashi K, Yoneda M, Imajo K, Tomeno W, Nakaya A, Suzuki Y, Saito S, Nakajima A.** Identification of core gene networks and hub genes associated with progression of non-alcoholic fatty liver disease by RNA sequencing. *Hepatol Res* 47: 1445–1458, 2017. doi:10.1111/hepr.12877.
 23. **Juluri R, Vuppalanchi R, Olson J, Unalp A, Van Natta ML, Cummings OW, Tonascia J, Chalasani N.** Generalizability of the nonalcoholic steatohepatitis Clinical Research Network histologic scoring system for nonalcoholic fatty liver disease. *J Clin Gastroenterol* 45: 55–58, 2011. doi:10.1097/MCG.0b013e3181dd1348.
 24. **Käräjämäki AJ, Bloigu R, Kauma H, Kesäniemi YA, Koivurova O-P, Perkiömäki J, Huikuri H, Ukkola O.** Non-alcoholic fatty liver disease with and without metabolic syndrome: Different long-term outcomes. *Metabolism* 66: 55–63, 2017. doi:10.1016/j.metabol.2016.06.009.
 25. **Kleiner DE, Brunt EM, Van Natta M, Behling C, Contos MJ, Cummings OW, Ferrell LD, Liu Y-C, Torbenson MS, Unalp-Arida A, Yeh M, McCullough AJ, Sanyal AJ; Nonalcoholic Steatohepatitis Clinical Research Network.** Design and validation of a histological scoring system for nonalcoholic fatty liver disease. *Hepatology* 41: 1313–1321, 2005. doi:10.1002/hep.20701.
 26. **Kristiansen MNB, Veidal SS, Righolt KT, Tølbøl KS, Roth JD, Jelsing J, Vrang N, Feigh M.** Obese diet-induced mouse models of nonalcoholic steatohepatitis-tracking disease by liver biopsy. *World J Hepatol* 8: 673–684, 2016. doi:10.4254/wjh.v8.i16.673.
 27. **Lackner C, Gogg-Kamerer M, Zatloukal K, Stumptner C, Brunt EM, Denk H.** Ballooned hepatocytes in steatohepatitis: the value of keratin immunohistochemistry for diagnosis. *J Hepatol* 48: 821–828, 2008. doi:10.1016/j.jhep.2008.01.026.
 28. **Lefebvre P, Lalloyer F, Baugé E, Pawlak M, Gheeraert C, Dehondt H, Vanhoutte J, Woitrain E, Hennuyer N, Mazuy C, Bobowski-Gérard M, Zummo FP, Derudas B, Driessen A, Hubens G, Vonghia L, Kwanten WJ, Michielsen P, Vanwolleghem T, Eeckhoutte J, Verrijken A, Van Gaal L, Francque S, Staels B.** Interspecies NASH disease activity whole-genome profiling identifies a fibrogenic role of PPAR α -regulated dermatopontin. *JCI Insight* 2: 92264, 2017. doi:10.1172/jci.insight.92264.
 29. **Liu FT, Hsu DK, Zuberi RI, Kuwabara I, Chi EY, Henderson WR Jr.** Expression and function of galectin-3, a beta-galactoside-binding lectin, in human monocytes and macrophages. *Am J Pathol* 147: 1016–1028, 1995.
 30. **Love MI, Huber W, Anders S.** Moderated estimation of fold change and dispersion for RNA-seq data with DESeq2. *Genome Biol* 15: 550, 2014. doi:10.1186/s13059-014-0550-8.
 31. **Machado MV, Michelotti GA, Pereira TA, Xie G, Premont R, Cortez-Pinto H, Diehl AM.** Accumulation of duct cells with activated YAP parallels fibrosis progression in non-alcoholic fatty liver disease. *J Hepatol* 63: 962–970, 2015. doi:10.1016/j.jhep.2015.05.031.
 32. **Marengo A, Rosso C, Bugianesi E.** Liver cancer: connections with obesity, fatty liver, and cirrhosis. *Annu Rev Med* 67: 103–117, 2016. doi:10.1146/annurev-med-090514-013832.
 33. **Matteoni CA, Younossi ZM, Gramlich T, Boparai N, Liu YC, McCullough AJ.** Nonalcoholic fatty liver disease: a spectrum of clinical and pathological severity. *Gastroenterology* 116: 1413–1419, 1999. doi:10.1016/S0016-5085(99)70506-8.
 34. **Mota M, Banini BA, Cazanave SC, Sanyal AJ.** Molecular mechanisms of lipotoxicity and glucotoxicity in nonalcoholic fatty liver disease. *Metabolism* 65: 1049–1061, 2016. doi:10.1016/j.metabol.2016.02.014.
 35. **Moylan CA, Pang H, Dellinger A, Suzuki A, Garrett ME, Guy CD, Murphy SK, Ashley-Koch AE, Choi SS, Michelotti GA, Hampton DD, Chen Y, Tillmann HL, Hauser MA, Abdelmalek MF, Diehl AM.** Hepatic gene expression profiles differentiate presymptomatic patients with mild versus severe nonalcoholic fatty liver disease. *Hepatology* 59: 471–482, 2014. doi:10.1002/hep.26661.
 36. **Neuschwander-Tetri BA.** Hepatic lipotoxicity and the pathogenesis of nonalcoholic steatohepatitis: the central role of nonglyceride fatty acid metabolites. *Hepatology* 52: 774–788, 2010. doi:10.1002/hep.23719.
 37. **Pereira TA, Xie G, Choi SS, Syn W-K, Voietta I, Lu J, Chan IS, Swiderska M, Amaral KB, Antunes CM, Secor WE, Witek RP, Lambertucci JR, Pereira FL, Diehl AM.** Macrophage-derived Hedge-

- hog ligands promotes fibrogenic and angiogenic responses in human schistosomiasis mansoni. *Liver Int* 33: 149–161, 2013. doi:10.1111/liv.12016.
38. Rangwala F, Guy CD, Lu J, Suzuki A, Burchette JL, Abdelmalek MF, Chen W, Diehl AM. Increased production of sonic hedgehog by ballooned hepatocytes. *J Pathol* 224: 401–410, 2011. doi:10.1002/path.2888.
 39. Ritchie ME, Phipson B, Wu D, Hu Y, Law CW, Shi W, Smyth GK. limma powers differential expression analysis for RNA-sequencing and microarray studies. *Nucleic Acids Res* 43: e47, 2015. doi:10.1093/nar/gkv007.
 40. Rosso N, Chavez-Tapia NC, Tiribelli C, Bellentani S. Translational approaches: from fatty liver to non-alcoholic steatohepatitis. *World J Gastroenterol* 20: 9038–9049, 2014. doi:10.3748/wjg.v20.i27.9038.
 41. Ryaboshapkina M, Hammar M. Human hepatic gene expression signature of non-alcoholic fatty liver disease progression, a meta-analysis. *Sci Rep* 7: 12361, 2017. doi:10.1038/s41598-017-10930-w.
 42. Shubham K, Vinay L, Vinod PK. Systems-level organization of non-alcoholic fatty liver disease progression network. *Mol Biosyst* 13: 1898–1911, 2017. doi:10.1039/C7MB00013H.
 43. Singh S, Allen AM, Wang Z, Prokop LJ, Murad MH, Loomba R. Fibrosis progression in nonalcoholic fatty liver vs nonalcoholic steatohepatitis: a systematic review and meta-analysis of paired-biopsy studies. *Clin Gastroenterol Hepatol* 13: 643–54.e9, 2015. doi:10.1016/j.cgh.2014.04.014.
 44. Smalling RL, Delker DA, Zhang Y, Nieto N, McGuinness MS, Liu S, Friedman SL, Hagedorn CH, Wang L. Genome-wide transcriptome analysis identifies novel gene signatures implicated in human chronic liver disease. *Am J Physiol Gastrointest Liver Physiol* 305: G364–G374, 2013. doi:10.1152/ajpgi.00077.2013.
 45. Starmann J, Fälth M, Spindelböck W, Lanz K-L, Lackner C, Zatloukal K, Trauner M, Sültmann H. Gene expression profiling unravels cancer-related hepatic molecular signatures in steatohepatitis but not in steatosis. *PLoS One* 7: e46584, 2012. doi:10.1371/journal.pone.0046584.
 46. Syn W-K, Jung Y, Omenetti A, Abdelmalek M, Guy CD, Yang L, Wang J, Witek RP, Fearing CM, Pereira TA, Teaberry V, Choi SS, Conde-Vancells J, Karaca GF, Diehl AM. Hedgehog-mediated epithelial-to-mesenchymal transition and fibrogenic repair in nonalcoholic fatty liver disease. *Gastroenterology* 137: 1478–1488.e8, 2009. doi:10.1053/j.gastro.2009.06.051.
 47. Tilg H, Moschen AR, Roden M. NAFLD and diabetes mellitus. *Nat Rev Gastroenterol Hepatol* 14: 32–42, 2017. doi:10.1038/nrgastro.2016.147.
 48. Tobin NP, Foukakis T, De Petris L, Bergh J. The importance of molecular markers for diagnosis and selection of targeted treatments in patients with cancer. *J Intern Med* 278: 545–570, 2015. doi:10.1111/joim.12429.
 49. Våremo L, Nielsen J, Nookaew I. Enriching the gene set analysis of genome-wide data by incorporating directionality of gene expression and combining statistical hypotheses and methods. *Nucleic Acids Res* 41: 4378–4391, 2013. doi:10.1093/nar/gkt111.
 50. Wang X-C, Zhan X-R, Li X-Y, Yu J-J, Liu X-M. Identification and validation co-differentially expressed genes with NAFLD and insulin resistance. *Endocrine* 48: 143–151, 2015. doi:10.1007/s12020-014-0247-5.
 51. Wong RJ, Aguilar M, Cheung R, Perumpail RB, Harrison SA, Younossi ZM, Ahmed A. Nonalcoholic steatohepatitis is the second leading etiology of liver disease among adults awaiting liver transplantation in the United States. *Gastroenterology* 148: 547–555, 2015. doi:10.1053/j.gastro.2014.11.039.
 52. Wruck W, Kashofer K, Rehman S, Daskalaki A, Berg D, Gralka E, Jozefczuk J, Drews K, Pandey V, Regenbrecht C, Wierling C, Turano P, Korf U, Zatloukal K, Lehrach H, Westerhoff HV, Adjaye J. Multi-omic profiles of human non-alcoholic fatty liver disease tissue highlight heterogenic phenotypes. *Sci Data* 2: 150068, 2015. doi:10.1038/sdata.2015.68.
 53. Younossi Z, Anstee QM, Marietti M, Hardy T, Henry L, Eslam M, George J, Bugianesi E. Global burden of NAFLD and NASH: trends, predictions, risk factors and prevention. *Nat Rev Gastroenterol Hepatol* 15: 11–20, 2018. doi:10.1038/nrgastro.2017.109.
 54. Younossi ZM, Baranova A, Ziegler K, Del Giacco L, Schlauch K, Born TL, Elariny H, Gorreta F, VanMeter A, Younoszai A, Ong JP, Goodman Z, Chandhoke V. A genomic and proteomic study of the spectrum of nonalcoholic fatty liver disease. *Hepatology* 42: 665–674, 2005. doi:10.1002/hep.20838.
 55. Younossi ZM, Gorreta F, Ong JP, Schlauch K, Del Giacco L, Elariny H, Van Meter A, Younoszai A, Goodman Z, Baranova A, Christensen A, Grant G, Chandhoke V. Hepatic gene expression in patients with obesity-related non-alcoholic steatohepatitis. *Liver Int* 25: 760–771, 2005. doi:10.1111/j.1478-3231.2005.01117.x.
 56. Younossi ZM, Gramlich T, Liu YC, Matteoni C, Petrelli M, Goldblum J, Rybicki L, McCullough AJ. Nonalcoholic fatty liver disease: assessment of variability in pathologic interpretations. *Mod Pathol* 11: 560–565, 1998.
 57. Younossi ZM, Koenig AB, Abdelatif D, Fazel Y, Henry L, Wymer M. Global epidemiology of nonalcoholic fatty liver disease—meta-analytic assessment of prevalence, incidence, and outcomes. *Hepatology* 64: 73–84, 2016. doi:10.1002/hep.28431.
 58. Zhu R, Baker SS, Moylan CA, Abdelmalek MF, Guy CD, Zamboni F, Wu D, Lin W, Liu W, Baker RD, Govindarajan S, Cao Z, Farci P, Diehl AM, Zhu L. Systematic transcriptome analysis reveals elevated expression of alcohol-metabolizing genes in NAFLD livers. *J Pathol* 238: 531–542, 2016. doi:10.1002/path.4650.